Materials Letters 185 (2016) 13–16

Contents lists available at ScienceDirect

Materials Letters

journal homepage: www.elsevier.com/locate/matlet

Layer thickness and sequence effects on resonant magnetoelectric coupling in $Ni/Pb(Zr,Ti)O_3$ cylindrical composites

Lirong Xu [a], Yu Yan [a], Lijie Qiao [a], Jiao Wang [a], De'an Pan [b,*], Song Yang [c], Alex A. Volinsky [c]

[a] Corrosion and Protection Center, Key Laboratory for Environmental Fracture (MOE), University of Science and Technology Beijing, Beijing, 100083 PR China
[b] Institute of Circular Economy, Beijing University of Technology, Beijing, 100124 PR China
[c] Department of Mechanical Engineering, University of South Florida, Tampa, FL, 33620 USA

ARTICLE INFO

Article history:
Received 17 May 2016
Received in revised form
27 July 2016
Accepted 10 August 2016
Available online 10 August 2016

Keywords:
Composite materials
Magnetoelectric
Electrodeposition
Thickness
Layer sequence

ABSTRACT

$Ni/Pb(Zr,Ti)O_3/Ni$, $Ni/Pb(Zr,Ti)O_3$ and $Pb(Zr,Ti)O_3/Ni$ cylindrical layered magnetoelectric (ME) composites with different Ni layer thickness were prepared by electrodeposition. The resonant ME effect was studied in both axial and vertical modes. The optimal DC magnetic field increases with Ni layer thickness and resonant ME voltage coefficients are maximum at intermediate Ni layer thickness for all cases. The resonant ME effect is also influenced by magnetostrictive and piezoelectric layer sequence. The $Pb(Zr,Ti)O_3/Ni$ cylinder has the best ME performance because of the highest axial ME voltage coefficient, almost highest vertical ME voltage coefficient and lowest optimal DC magnetic field in both modes. This work provides guidance to optimize ME performance in cylindrical layered ME composites.

1. Introduction

Magnetoelectric (ME) effect is the coupling between electric polarization and magnetization. In magnetostrictive-piezoelectric composite, the ME effect is dominated by the strain transfer at phase interfaces [1,2]. Layered ME composites show the strongest ME effect and have been utilized for many device technologies, including ME sensors, energy harvesters and so on [3–6]. Compared with plate composites, cylindrical layered ME composites have more compact structure, which is beneficial for device miniaturization. On the other hand, due to the self-bound effect of the cylindrical structure, both the piezoelectric (PE) modes of d_{31} and d_{33} of the PE phase combine together to induce better ME coupling [7]. It has been demonstrated that Ni and $Pb(Zr,Ti)O_3$ (PZT) cylindrical layered composites made by electrodeposition have giant ME coupling due to rigid and direct contact at interfaces without the use of adhesives [8,9].

A few studies have investigated the influence of various factors, such as geometry, boundary conditions and imperfect interface of cylindrical layered ME composites on the ME effect [7–14]. Wu et al. [7] presented the theoretical model of long trilayer and bilayer cylindrical ME composites to predict the resonant ME response. For the finite length ME composite cylinder, a three-dimensional exact solution under simply-supported boundary conditions was obtained [10]. However, this work only discussed the axial ME effect related to length and curvature. Wang et al. [11,12] applied uniform radial magnetic field to derive an analytical solution for the ME effect in bilayer cylinder. However, uniform radial magnetic field is uncommon in ME device applications. Other experimental studies have reported the diameter and length effects on the ME properties of cylindrical composites [13,14]. However, only a few experiments have focused on the layer sequence of the PE and magnetostrictive (MS) layers and the MS layer thickness effects.

In this work, Ni/PZT/Ni, Ni/PZT and PZT/Ni cylindrical layered ME composites are electrodeposited for comparison. The ME effect can be amplified in resonance by the quality factor Q, which improves ME devices performance [5]. Moreover, static and resonant ME responses of ME composites do not always have identical trends with changing parameters [11–14]. Given these, the resonant frequency and corresponding resonant ME effect dependence on the MS Ni layer thickness are investigated. The effect of the layer sequence is also discussed.

2. Experiment

Three samples with the abovementioned layer sequences were prepared by electrodeposition, as shown schematically in Fig. 1. The three PZT ceramic rings with the $\Phi 20 \times \Phi 18 \times 10\ mm^3$

* Corresponding author.
E-mail address: pandean@bjut.edu.cn (D. Pan).

http://dx.doi.org/10.1016/j.matlet.2016.08.042
0167-577X/

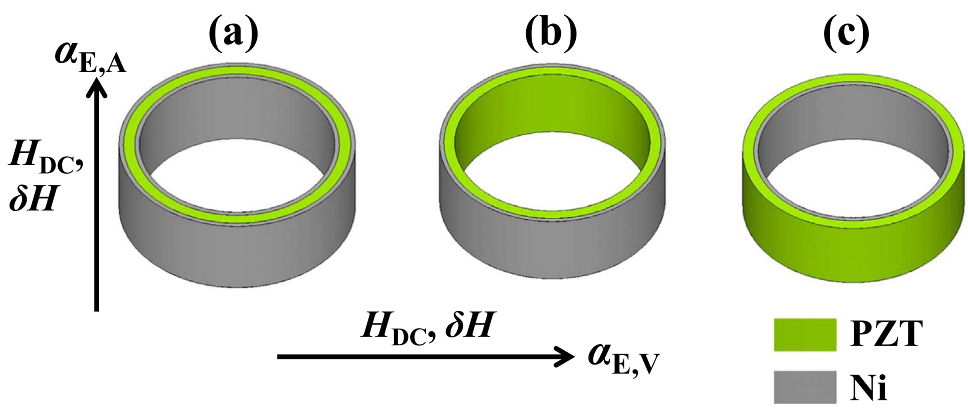

Fig. 1. Schematics of: (a) Ni/PZT/Ni, (b) Ni/PZT and (c) PZT/Ni cylindrical layered ME composites.

dimensions were radially polarized. First, Ni was electrodeposited on each PZT sample for four hours. Ni electrodeposition bath composition and conditions are described elsewhere [8]. With the same electrodeposition time, all Ni layers thickness, t_m, was approximately 200 μm. Then for each sample, the ME properties were characterized. The four-hour electrodeposition and ME measurements were continued for the three samples three more times. The corresponding successive t_m was about 400 μm, 600 μm and 800 μm. The ME characterization was performed in the ME measurement system. With both DC (H_{DC}) and alternating (δH) magnetic field applied parallel (axial mode) or perpendicular (vertical mode) to the cylinder axis, two corresponding ME voltage coefficients, $\alpha_{E,A}$ and $\alpha_{E,V}$, were obtained. The ME voltage coefficient was calculated as $\alpha_E = \delta V/(t_{PZT} \cdot \delta H)$, where t_{PZT} is the PZT thickness and δH is the amplitude of the AC magnetic field generated by the Helmholtz coils.

3. Results and discussion

Fig. 2 shows the AC magnetic field frequency, f, dependence of $\alpha_{E,A}$ for the Ni/PZT/Ni, Ni/PZT and PZT/Ni cylinders in axial mode with increasing Ni layer thickness t_m=200, 400, 600 and 800 μm. For all cases, the samples were measured under their corresponding optimal DC magnetic field H_m. Obviously, the ME voltage output is analogous for all three samples with different t_m. There are two resonant peaks in all cases, even though the second peaks for the PZT/Ni cylinder are rather weak (see Fig. 2(c)).

For the three samples with various t_m in the vertical mode, the $\alpha_{E,V}$ dependence on f is presented in Fig. 3. The ME voltage output shows similar trends with the axial mode. Both the maximum $\alpha_{E,A}$ and $\alpha_{E,V}$ are observed at the first resonant peak, which will be discussed further. As shown in Figs. 2 and 3, the first peaks of t_m=200 μm samples are quite close to 50 kHz. Meanwhile, the resonant α_E peak of an ME composite is at the electromechanical anti-resonance frequency (f_a) of the piezoelectric layer [15–17]. Anti-resonance frequencies of the radial vibration mode of the three PZT rings were provided by the manufacturer as 49.5, 48.6 and 49.1 kHz, respectively. It can be inferred that the first resonant peaks correspond to the radial extension vibration modes of the three cylinders.

To better understand the resonant ME effect, Fig. 4 shows the Ni layer thickness t_m dependence of the maximum resonant ME voltage coefficient $\alpha_{E,max}$ and the optimal DC magnetic field H_m for the three samples in both axial and vertical modes. Both $\alpha_{E,max}$ and H_m strongly depend on t_m. Therefore, proper t_m is essential for the ME performance. H_m monotonously increases with t_m in all cases. In the axial mode, the three samples exhibit the best ME voltage outputs when t_m ranges from 200 μm to 400 μm. The maximum resonant $\alpha_{E,A}$ of the PZT/Ni cylinder with various t_m are higher than the Ni/PZT/Ni and Ni/PZT cylinders, while H_m is the lowest. Since the magnetostrictive coefficient of the Ni layer is negative, it shrinks along the axial direction and expands along the circumferential direction when the external magnetic field is applied in the axial mode. Note that the Ni ring thickness is much less than the radius, so the stress and strain in the radial direction can be ignored. Thus, axial compressive and circumferential tensile stresses are transformed to the PZT ring [18]. For the radial extension vibration mode, the Ni layer on the inner surface of the PZT ring is superior to the outer surface, since Ni layer on the outer surface can hinder radial extension. Since the outer surface of the PZT ring in the PZT/Ni cylinder is free, the ME coupling is more efficient in the PZT/Ni cylinder. These results suggest that in the axial mode the PZT/Ni cylinder would have the best ME performance.

In the vertical mode, the optimal t_m of $\alpha_{E,V}$ for the three samples ranges from 400 μm to 600 μm. When external magnetic field is applied in the vertical mode, radial and circumferential stresses are present in the PZT rings. When $t_m < 600$ μm, the maximum $\alpha_{E,V}$ of the Ni/PZT/Ni cylinder is the highest. This can be attributed to the fact that the radial stresses of the inner and outer Ni layers can cancel each other, while both circumferential stresses of the two layers contribute to the ME effect. However, the maximum $\alpha_{E,V}$ of the PZT/Ni cylinder is higher than the Ni/PZT/Ni cylinder at $t_m \geq 600$ μm. This phenomenon is mainly due to the large enough radial compressive stress for thicker t_m. The appearance of dual peak for the Ni/PZT cylinder can be attributed to flexural strain induced by the asymmetric structure of the bilayer composite [7]. In view of the above, the PZT/Ni cylinder is most suitable for practical applications according to its advantages in reducing weight, but having nearly the highest ME output. On the other hand, H_m of the PZT/Ni cylinder is also the lowest in the vertical mode, which reinforces the previous statement.

4. Conclusions

In conclusion, the resonant magnetoelectric effect in three different layer sequenced Ni and $Pb(Zr,Ti)O_3$ cylindrical layered composites with different Ni layer thickness, prepared by electrodeposition, was investigated. Experimental results indicate that the optimal DC magnetic field increases with Ni layer thickness, while resonant ME voltage coefficients achieve maximum value with intermediate Ni layer thickness for all three Ni/PZT/Ni, Ni/PZT and PZT/Ni cylinders. The ME effect in the PZT/Ni cylinder is better when both the ME voltage coefficient and optimal DC magnetic field are considered. This work provides guidance for designing cylindrical layered ME composites.

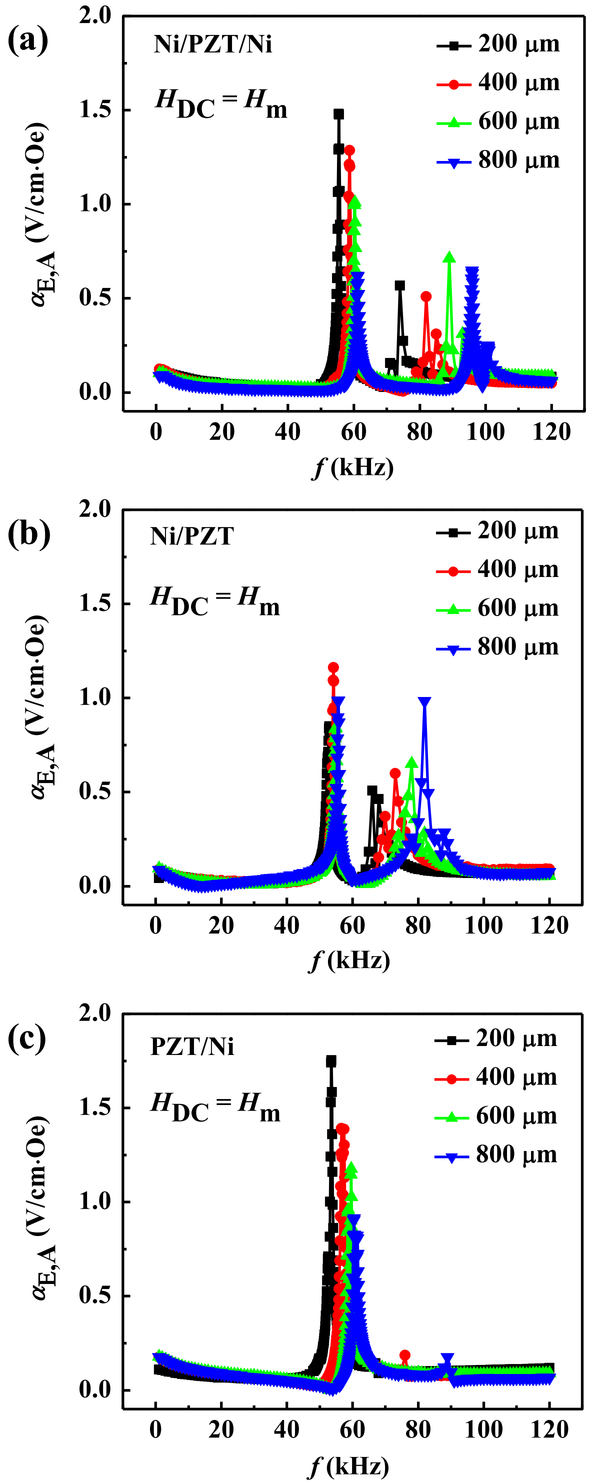

Fig. 2. The ME voltage coefficient $\alpha_{E,A}$ dependence on the AC magnetic field frequency f for: (a) Ni/PZT/Ni, (b) Ni/PZT and (c) PZT/Ni cylinders with various Ni layer thickness.

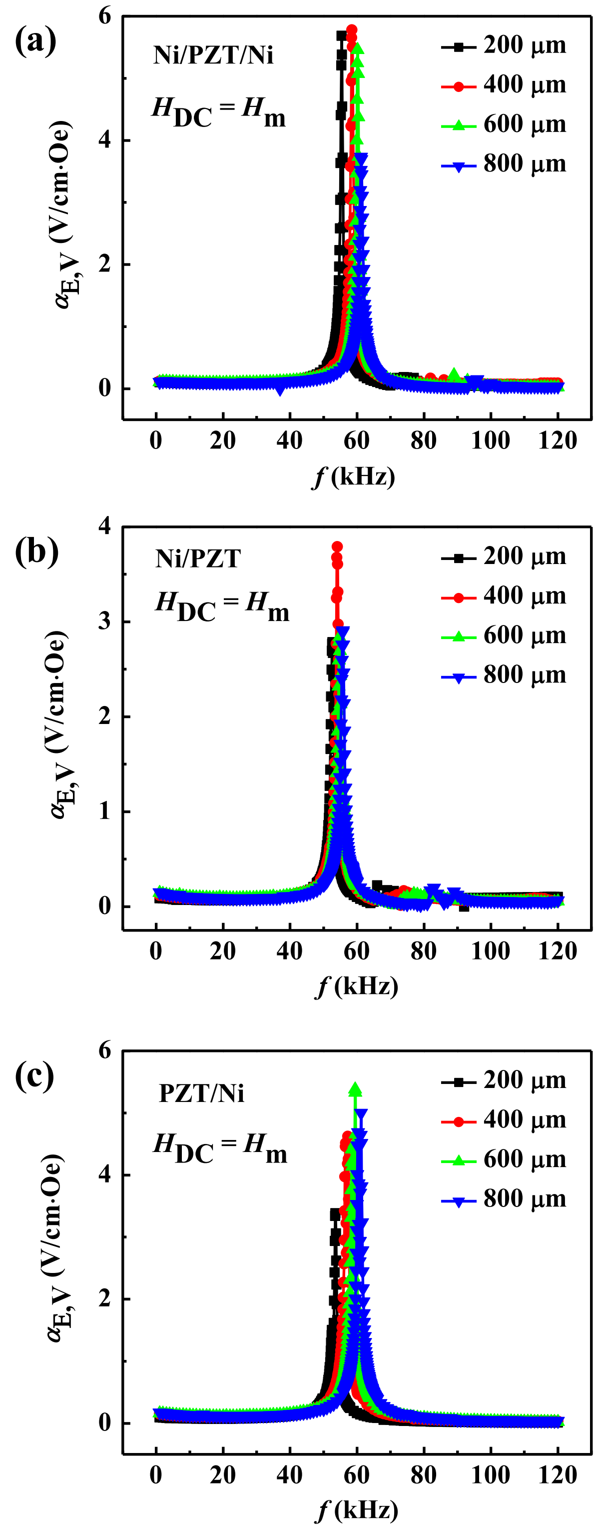

Fig. 3. The ME voltage coefficient $\alpha_{E,V}$ dependence on the AC magnetic field frequency f for: (a) Ni/PZT/Ni, (b) Ni/PZT and (c) PZT/Ni cylinders with various Ni layer thickness.

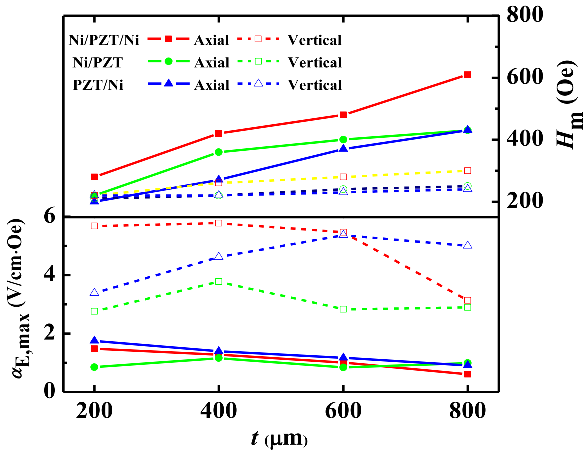

Fig. 4. The maximum resonant ME voltage coefficient $\alpha_{E,max}$ and the optimal DC magnetic field H_m dependence on the Ni layer thickness for Ni/PZT/Ni, Ni/PZT and PZT/Ni cylinders in axial and vertical modes.

Acknowledgments

This work was supported by the Beijing Nova Program (Z141103001814006) and the Fundamental Research Funds for the Central Universities (Project No: FRF-TP-14-001C1).

References

[1] W. Eerenstein, N.D. Mathur, J.F. Scott, Nature 442 (2006) 759–765.
[2] J.M. Hu, L.Q. Chen, C.W. Nan, Adv. Mater. 28 (2016) 15–39.
[3] J. Gao, Y. Wang, M. Li, Y. Shen, J. Li, D. Viehland, Mater. Lett. 85 (2012) 84–87.
[4] J. Ryu, D.Y. Jeong, et al., Energy Environ. Sci. 8 (2015) 2402.
[5] J.F. Scott, J. Mater. Chem. 22 (2012) 4567–4574.
[6] J. Zhai, Z. Xing, S. Dong, J. Li, D. Viehland, J. Am. Ceram. Soc. 91 (2) (2008) 351–358.
[7] G. Wu, R. Zhang, L. Zhang, H. Zhu, N. Zhang, J. Appl. Phys. 113 (2013) 214105.
[8] D.A. Pan, Y. Bai, A.A. Volinsky, W.Y. Chu, L.J. Qiao, Appl. Phys. Lett. 92 (2008) 052904.
[9] D.A. Pan, J. Wang, et al., Mater. Lett. 133 (2014) 255–258.
[10] Y. Huang, D.Z. Liu, Int. J. Mech. Sci. 76 (2013) 158–165.
[11] H.M. Wang, E. Pan, W.Q. Chen, J. Appl. Phys. 107 (2010) 093514.
[12] H.M. Wang, E. Pan, W.Q. Chen, Phys. Status Solidi B 248 (9) (2011) 2180–2185.
[13] K. Bi, W. Wu, Q.L. Gu, H.N. Cui, Y.G. Wang, J. Alloy. Compd. 509 (2011) 5163–5166.
[14] D. Xie, Y.G. Wang, J.H. Cheng, J. Alloy. Compd. 615 (2014) 298–301.
[15] Y. Jia, H. Luo, X. Zhao, F. Wang, Adv. Mater. 20 (2008) 4776–4779.
[16] Z. Wu, Z. Xiang, Y. Jia, Y. Zhang, H. Luo, Appl. Phys. Lett. 112 (2012) 106102.
[17] G. Wu, T. Nan, R. Zhang, N. Zhang, S. Li, N.X. Sun, Appl. Phys. Lett. 103 (2013) 182905.
[18] W.Q. Jing, F. Fang, Appl. Phys. Lett. 106 (2015) 212901.